

A Performance and Improvement of Optimal Voltage Control Scheme for Three-Phase Ups Systems

A.Nayomi

M.Tech (EPS),

Arjun College of Technology and Sciences.

S.Chandra Mouli, M.Tech

Assistant Professor,

Arjun College of Technology and Sciences.

ABSTRACT:

This paper proposes a straightforward ideal voltage control strategy for three-stage uninterruptible-power-sup-employ frameworks. The proposed voltage controller is made out of a criticism control term and a remunerating control term. The previous term is intended to make the framework mistakes join to zero, though the last term is connected to make up for the framework vulnerabilities. Besides, the ideal burden current eyewitness is utilized to enhance sys-tem expense and unwavering quality. Especially, the shut circle steadiness of an eyewitness based ideal voltage control law is scientifically demonstrated by demonstrating that the entire conditions of the increased onlooker based control framework blunders exponentially unite to zero. Not at all like past calculations, can the proposed strategy make a tradeoff between control information extent and following mistake by essentially picking legitimate execution lists. The adequacy of the proposed controller is approved through reproductions on MATLAB/Simulink and investigates a model 600-VA tried with a TMS320LF28335 DSP. At long last, the similar results for the proposed plan and the customary criticism linearization control plan are exhibited to show that the proposed calculation accomplishes a brilliant execution, for example, quick transient reaction, little enduring state mistake, and low aggregate consonant contortion under burden step change, lopsided burden, and nonlinear burden with the parameter varieties.

Index Terms:

Optimal load current observer, optimal voltage control, three-phase inverter, total harmonic distortion (THD), uninterruptible power supply (UPS).

I. INTRODUCTION:

Uninterruptible force supply (UPS) frameworks supply crisis power if there should arise an occurrence of utility force disappointments. As of late, the significance of the UPS frameworks has been escalated increasingly because of the expansion of touchy and basic applications, for example, correspondence frameworks, restorative hardware, semiconductor fabricating frameworks, and information handling frameworks [1]–[3]. These applications require clean power and high unwavering quality paying little respect to the electric force disappointments and misshaped utility supply voltage. In this manner, the execution of the UPS frameworks is typically assessed as far as the aggregate consonant mutilation (THD) of the yield voltage and the transient/relentless state reactions paying little respect to the heap conditions: load step change, straight load, and nonlinear burden [4]–[7]. To enhance the previously mentioned execution records, various control calculations have been proposed, for example, proportional–integral (PI) control, H_{∞} circle molding control, model prescient control, bum control, sliding-mode control, dull control, versatile control, and criticism linearization control (FLC). The customary PI control proposed in [8] and [9] is anything but difficult to actualize; be that as it may, the THD estimation of the yield voltage is not low under a nonlinear-load condition. In [10], the H_{∞} circle forming control plan is depicted and actualized on a solitary stage inverter, which has a straightforward structure and is vigorous against model vulnerabilities. A model prescient control technique for UPS applications is portrayed in [11]. By utilizing a heap current eyewitness as a part of spot of current sensors, the creators guaranteed a decreased framework cost.

Be that as it may, the recreation and test comes about don't uncover an excellent execution as far as THD and unflinching state mistake. In [12], the miscreant control strategy utilizes the state criticism data to make up for the voltage drop over the inductor. Notwithstanding, this strategy shows affectability to parameter befuddles, and the sounds of the inverter yield voltage are not extremely all around adjusted. In [13] and [14], the sliding-mode control procedure reflects heartiness to the framework commotion, and still, the control framework has an outstanding jabbering issue. In [15], dull control is connected to accomplish a brilliant sinusoidal yield voltage of a three-stage UPS framework. For the most part, this control system has a moderate reaction time. In [16], the versatile control technique with low THD is proposed; in any case, there is still a danger of uniqueness if the controller increases are not appropriately chose. Multivariable FLC is exhibited in [17]. In this control method, the nonlinearity of the framework is considered to accomplish low THD under nonlinear burden. Be that as it may, it is difficult to complete because of the calculation complexities. Thus, the up to specified direct controllers are straightforward, yet the execution is not agreeable under nonlinear burden. Interestingly, the nonlinear controllers have an exceptional execution, yet the usage is difficult because of the moderately confounded controllers. As such, the ideal control hypothesis has been inquired about in different fields, for example, aviation, financial matters, material science, thus on [18], since it has a calculable arrangement called an execution file that can quantitatively assess the framework execution by stand out from other control speculations. Also, the ideal control plan gives the optimality of the controller as indicated by a quadratic execution measure and empowers the control framework to have great properties, for example, enough pick up and stage edge, vigor to instabilities, great resistance of nonlinearities, and so on [19]. Subsequently, a direct ideal controller has not just a basic structure in examination with different controllers additionally a striking control execution like other nonlinear controllers [20]–[22].

Consequently, this paper proposes a spectator based ideal voltage control plan for three-stage UPS frameworks. This proposed voltage controller embodies two primary parts: an input control term and a remunerating control term. The previous term is intended to make the framework blunders unite to zero, and the last term is connected to appraise the framework instabilities. The Lyapunov hypothesis is utilized to investigate the strength of the framework. Exceptionally, this paper demonstrates the shut circle security of an eyewitness based ideal voltage control law by demonstrating that the framework mistakes exponentially meet to zero. Additionally, the proposed control law can be methodically outlined contemplating a tradeoff between control information sizes and following blunder dissimilar to past calculations [23]. The adequacy of the proposed control strategy is confirmed by means of recreations on MATLAB/Simulink and investigates a model 600-VA UPS inverter proving ground with a TMS320LF28335 DSP. In this paper, a traditional FLC strategy in [17] is chosen to exhibit the near results since it has a decent execution under a nonlinear-load condition, and its circuit model of a three-stage inverter in [17] is like our framework model. At long last, the outcomes plainly demonstrate that the proposed plan has a decent voltage control ability, for example, quick transient conduct, little enduring state blunder, and low THD under different burden conditions, for example, load step change, lopsided burden, and nonlinear burden in the presence of the parameter varieties.

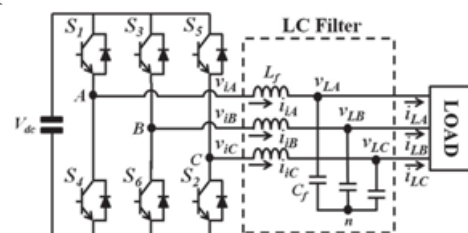


Fig. 1. Three-phase inverter with an LC filter for a UPS system.

II. SYSTEM DESCRIPTION AND PROBLEM FORMULATION

The three-stage UPS framework with a LC channel is appeared in Fig. 1, which is made out of a dc-join voltage (Vdc), a three-stage beat width adjustment (PWM) inverter (S1~S6), a yield LC channel (Lf, Cf), and a three-stage load (e.g., direct or nonlinear burden).

$$\begin{cases} \dot{i}_{id} = \omega i_{iq} + k_2 v_{id} - k_2 v_{Ld} & \dot{v}_{Ld} = \omega v_{Lq} + k_1 i_{id} - k_1 i_{Ld} \\ \dot{i}_{iq} = -\omega i_{id} + k_2 v_{iq} - k_2 v_{Lq} & \dot{v}_{Lq} = -\omega v_{Ld} + k_1 i_{iq} - k_1 i_{Lq} \end{cases} \quad (1)$$

Based on Fig. 1, the dynamic model of a three-phase inverter can be derived in a d-q synchronous reference frame as follows [24]: Where $k_1 = 1/C_f$, and $k_2 = 1/L_f$. In system model (1), v_{Ld} , v_{Lq} , i_{id} , and i_{iq} are the state variables, and v_{id} and v_{iq} are the control inputs. In this scheme, the assumption is made to construct the optimal voltage controller and optimal load current observer as follows: The load currents (i_{Ld} and i_{Lq}) are unknown and vary very slowly during the sampling period [11].

III. PROPOSED OPTIMAL VOLTAGE CONTROLLER DESIGN AND STABILITY ANALYSIS

A. Optimal Voltage Controller Design

Here, a simple optimal voltage controller is proposed for system (1). First, let us define the d-q-axis inverter current references (i^*_{id} , i^*_{iq}) as

$$i^*_{id} = i_{Ld} - \frac{1}{k_1} \omega v^*_{Lq}, \quad i^*_{iq} = i_{Lq} + \frac{1}{k_1} \omega v^*_{Ld} \quad (2)$$

Then, the error values of the load voltages and inverter currents are set as

$$\begin{aligned} v_{de} &= v_{Ld} - v_{Ld}^*, & v_{qe} &= v_{Lq} - v_{Lq}^* \\ i_{de} &= i_{id} - i_{id}^*, & i_{qe} &= i_{iq} - i_{iq}^* \end{aligned} \quad (3)$$

Therefore, system model (1) can be transformed into the following error dynamics:

$$x' = Ax + B(u + ud) \quad (4)$$

where $x = [v_{de} \ v_{qe} \ i_{de} \ i_{qe}]^T$, $u = [v_{id} \ v_{iq}]^T$, $ud = [d_d \ d_q]^T$,

$$A = \begin{bmatrix} 0 & \omega & k_1 & 0 \\ -\omega & 0 & 0 & k_1 \\ -k_2 & 0 & 0 & 0 \\ 0 & -k_2 & 0 & 0 \end{bmatrix}, \quad B = \begin{bmatrix} 0 & 0 \\ 0 & 0 \\ k_2 & 0 \\ 0 & k_2 \end{bmatrix}$$

$d_q = -v^*_{Ld} + (1/k_2)\omega i_{Lq}$, and $d_d = -v^*_{Lq} + (1/k_2)\omega i_{Ld}$.

Note that ud is applied to compensate for the system uncertainties as a compensating term.

Consider the following Riccati equation for the solution matrix P [25]:

$$PA + ATP - PBR^{-1}BTP + Q = 0 \quad (5)$$

Where Q and R are the positive definite weighting matrices with sufficient dimensions. Remark 1: Recall that Q and R are the weighting matrices [26]. Excessive large error or control input values can be penalized by using properly chosen Q and R. Generally, the large Q means a high control performance, whereas the large R means a small input magnitude. Consequently, there is a tradeoff between Q and R in the control system. The Q and R Parameters generally need to be tuned until satisfactory control results are obtained.

Let the diagonal matrices Q and R be defined as

$$Q = \begin{bmatrix} Q_1 & 0 & 0 & \dots & 0 \\ 0 & Q_2 & 0 & \dots & 0 \\ \dots & \dots & \dots & \dots & \dots \\ 0 & \dots & \dots & 0 & Q_m \end{bmatrix}$$

$$R = \begin{bmatrix} R_1 & 0 & 0 & \dots & 0 \\ 0 & R_2 & 0 & \dots & 0 \\ \dots & \dots & \dots & \dots & \dots \\ 0 & \dots & \dots & 0 & R_k \end{bmatrix}$$

where Q and R have positive diagonal entries such that $\sqrt{Q_i} = 1/y_{maxi}$, where $i = 1, 2, \dots, m$, and $\sqrt{R_i} = 1/u_{maxi}$, where $i = 1, 2, \dots, m$. The number y_{maxi} is the maximally acceptable deviation value for the i th component of output y . The other quantity u_{maxi} is the i th component of input u . With an initial guessed value, the diagonal entries of Q and R can be adjusted through a trial-and-error method. Then, the optimal voltage controller can be designed by the following equation:

$$u = -ud + Kx \quad (6)$$

Where $K = -R^{-1}B^T P$ denotes the gain matrix, and $u_{dand} Kx$ represent a feed forward control term and a feedback control term, respectively. Remark 2: The proposed voltage controller, in essence, is designed based on the well-known linear quadratic regulator minimizing the following performance index [27]:

$$J = \int_0^{\infty} (x^T Q x + u_n^T R u_n) dt \quad (7)$$

Where x is the error, $u = u + u_d$, and Q and R are symmetrical positive definite matrices as mentioned above.

B. Stability Analysis of Voltage Controller

Consider the following Lyapunov function:

$$V(x) = x^T P x. \quad (8)$$

From (4)–(6), and (8), the time derivative of $V(x)$ is given by the following

$$\begin{aligned} \dot{V}(x) &= \frac{d}{dt} x^T P x = 2x^T P(A + BK)x \\ &= 2x^T P(A - BR^{-1}B^T P)x \\ &= x^T (PA + A^T P - 2PBR^{-1}B^T P)x \leq -x^T Qx. \end{aligned} \quad (9)$$

This implies that x exponentially converges to zero.

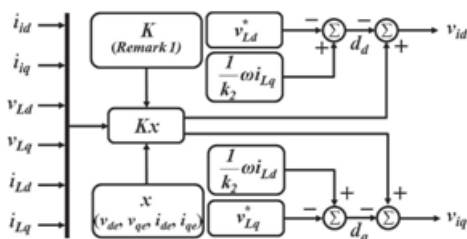


Fig. 2. Block diagram of the proposed optimal voltage control scheme.

Remark 3: By considering the parameter variations, the state-dependent coefficient matrix A is rewritten as $A = A + \Delta A$, where ΔA means the value of system parameter variations. Thus, (4) can be transformed into the following error dynamics

$$\dot{x} = A'x + B(u + u_d). \quad (10)$$

The new time derivative of (8) is given by the following:

$$\begin{aligned} \dot{V}(x) &= 2x^T P \dot{x} \\ &= x^T (PA + P\Delta A + \Delta A^T P + A^T P \\ &\quad - 2PBR^{-1}B^T P)x < 0. \end{aligned} \quad (11)$$

By (5), (11) is reduced to

$$V(x) = x^T (P\Delta A + \Delta A^T P - Q - PBRTBTP)x. \quad (12)$$

If the following inequality holds for the given ΔA :

$$P\Delta A + \Delta A^T P < PBR^{-1}BTP + Q \quad (13)$$

Then $\dot{V} < 0$ for all nonzero x . Therefore, the proposed optimal voltage control system can tolerate any parameter variation satisfying (13). Fig. 2 shows the block diagram of the proposed optimal voltage control scheme.

IV. OPTIMAL LOAD CURRENT OBSERVER DESIGN AND STABILITY ANALYSIS

A. Optimal Load Current Observer Design

As seen in (2) and (4), the inverter current references (i_d^* and i_q^*) and feed forward control term (u_d) need load current information as inputs. To avoid using current sensors, a linear optimal load current observer is introduced in this algorithm. From (1) and the assumption, the following dynamic models obtained to estimate the load current:

$$\begin{cases} \dot{x}_o = A_o x_o + B_o u_o \\ y = C_o x_o \end{cases} \quad (14)$$

$$\text{where } x_o = [i_{Ld} \ i_{Lq} \ v_{Ld} \ v_{Lq}]^T, \ u_o = [k_1 i_{id} \ k_1 i_{iq}]^T,$$

$$A_o = \begin{bmatrix} 0 & 0 & 0 & 0 \\ 0 & 0 & 0 & 0 \\ -k_1 & 0 & 0 & \omega \\ 0 & -k_1 & -\omega & 0 \end{bmatrix}, \ B_o = C_o^T = \begin{bmatrix} 0 & 0 \\ 0 & 0 \\ 1 & 0 \\ 0 & 1 \end{bmatrix}.$$

Then, the load current observer is expressed as

$$\dot{x}_o = A_o \hat{x}_o + B_o u_o - L(y - C_o \hat{x}_o) \quad (15)$$

Where $\hat{x}_0 = [\hat{i}_{Ld} \ \hat{i}_{Lq} \ \hat{v}_{Ld} \ \hat{v}_{Lq}]^T$, and \hat{i}_{Ld} and \hat{i}_{Lq} are estimates of i_{Ld} and i_{Lq} , respectively. In addition, L is an observer gain matrix calculated by

$$L = -P_o C_o^T R_o^{-1} \quad (16)$$

and P_o is the solution of the following Riccati equation:

$$A_o P_o + P_o A_o^T - P_o C_o^T R_o^{-1} C_o P_o + Q_o = 0 \quad (17)$$

Where Q_o and R_o are the positive definite weighting matrices with sufficient dimensions. The manner of choosing Q_o and R_o is the same as in Remark 1.

Remark 4: The fourth-order Kalman–Bucy optimal observer [19] is used to minimize the performance index $E(x^T e x_e)$, where $x_e = x_o - \hat{x}_o$, representing the expectation value of $x^T e x_e$ for the following perturbed model:

$$\dot{x}'_o = A_o x_o + B_o u + d, \quad y = C_o x_o + v \quad (18)$$

Where $d \in R^4$ and $v \in R^2$ are independent white Gaussian noise signals with $E(d) = 0$, $E(v) = 0$, $E(dd^T) = Q_o$, and $E(vv^T) = R_o$.

B. Stability Analysis of Load Current Observer

The error dynamics of the load current observer can be obtained as follows:

$$\dot{x}'_e = (A - LC)x_e. \quad (19)$$

Define the Lyapunov function as

$$V_o(x_e) = x_e^T X x_e \quad (20)$$

Where $X = P^{-1}o$. Its time derivative along the error dynamics (19) is represented by the following:

$$\begin{aligned} \dot{V}_o(\bar{x}) &= \frac{d}{dt} x_e^T X x_e = 2x_e^T (X A_o - X P_o C_o^T R_o^{-1} C_o) x_e \\ &= x_e^T X (A_o P_o + P_o A_o^T - 2P_o C_o^T R_o^{-1} C_o P_o) X x_e \\ &\leq -x_e^T X Q_o X x_e. \end{aligned} \quad (21)$$

This implies that x_e exponentially converges to zero.

V. OBSERVER-BASED CONTROL LAW AND CLOSED-LOOP STABILITY ANALYSIS

A. Observer-Based Control Law

With the estimated load currents achieved from the observer instead of the measured quantities, the inverter current errors and feedforward control term can be obtained as follows:

$$\begin{aligned} \bar{i}_{de} &= i_{id} - \hat{i}_{Ld} + \frac{1}{k_1} \omega v_{Lq}^*, \quad \bar{i}_{qe} = i_{iq} - \hat{i}_{Lq} - \frac{1}{k_1} \omega v_{Ld}^* \\ \bar{d}_d &= -v_{Ld}^* + \frac{1}{k_2} \omega \hat{i}_{Lq}, \quad \bar{d}_q = -v_{Lq}^* - \frac{1}{k_2} \omega \hat{i}_{Ld}. \end{aligned} \quad (22)$$

Then, (22) can be rewritten as the following equations:

$$\begin{aligned} \bar{i}_{de} &= i_{de} + [1 \ 0 \ 0 \ 0] x_e \\ \bar{i}_{qe} &= i_{qe} + [0 \ 1 \ 0 \ 0] x_e \\ \bar{d}_d &= d_d + \frac{\omega}{k_2} [0 \ 1 \ 0 \ 0] x_e \\ \bar{d}_q &= d_q - \frac{\omega}{k_2} [1 \ 0 \ 0 \ 0] x_e. \end{aligned} \quad (23)$$

From (6) and (23), the proposed observer-based control law can be achieved as

$$u = -\bar{u}_d + K \bar{x} \quad (24)$$

where $\bar{x} = [v_{de} \ v_{qe} \ \bar{i}_{de} \ \bar{i}_{qe}]^T$, and $\bar{u}_d = [\bar{d}_d \ \bar{d}_q]^T$.

B. Closed-Loop Stability Analysis

For the purpose of analyzing the stability, (24) is rewritten as the following:

$$u = -u_d + Kx + Hx_e \quad (25)$$

Where $H = (\omega/k_2) E + KF$, $\bar{x} = x + Fx_e$,

$$E = \begin{bmatrix} 0 & 1 & 0 & 0 \\ -1 & 0 & 0 & 0 \end{bmatrix}, \quad \text{and } F = \begin{bmatrix} 0 & 0 & 0 & 0 \\ 0 & 0 & 0 & 0 \\ 1 & 0 & 0 & 0 \\ 0 & 1 & 0 & 0 \end{bmatrix}$$

Let us define the Lyapunov equation as

$$V(x, x_e) = x^T P x + \zeta x_e^T P_o^{-1} x_e \quad (26)$$

where ζ is a scalar quantity that satisfies the following inequality:

$$\frac{\zeta > \|PBH\|^2}{[\lambda_{\min}(Q) \cdot \lambda_{\min}(P_o^{-1} Q_o P_o^{-1})]}. \quad (27)$$

Then, the time derivative of the Lyapunov equation is given by

$$\begin{aligned} \dot{V} &= 2x^T P(Ax + Bu + Bu_d) + 2\zeta x_e^T P_o^{-1} (A_o + LC_o) x_e \\ &= 2x^T P(Ax + BKx + BHx_e) + 2\zeta x_e^T P_o^{-1} (A_o + LC_o) x_e \\ &\leq -x^T Qx + 2x^T PBHx_e - \zeta x_e^T P_o^{-1} Q_o P_o^{-1} x_e \\ &\leq -\lambda_{\min}(Q) \|x\|^2 + 2\|PBH\| \cdot \|x\| \cdot \|x_e\| \\ &\quad - \zeta \lambda_{\min}(P_o^{-1} Q_o P_o^{-1}) \|x_e\|^2 \leq 0. \end{aligned} \quad (28)$$

This implies that x and x_e exponentially go to zero.

As a result, the design procedure of the proposed observer-based control law can be summarized as follows.

Step 1) Build system model (1) in the d–q coordinate frame and then derive error dynamics (4) by using system parameters.

Step 2) set the optimal voltage controller (6) with the feed-forward control term (u_d) and feedback control term (Kx).

Step 3) Define the load current estimation model (14) and build the load current observer (15) by using the Kalman–Bucy optimal observer.

Step 4) Select the observer weighting matrices Q_o and R_o in Riccati equation by referring to Remark 1. Then, choose the observer gain L in (16) using Q_o and R_o .

Step 5) Select the controller weighting matrices Q and R in Riccati equation by referring to Remark 1. Then, choose the control gain K in (6) using Q and R .

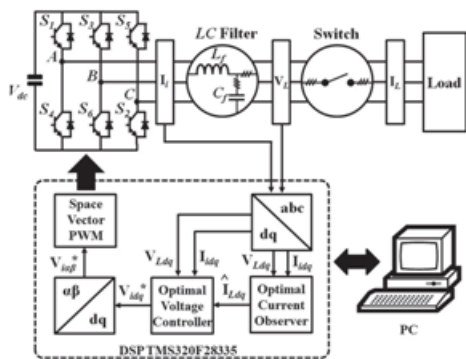


Fig. 3. Block diagram of the proposed observer-based optimal voltage control system.

TABLE I: SYSTEM PARAMETERS OF A 600-VA TESTBED

| Parameters | Descriptions | Values | Units |
|-------------|--------------------------------|--------|--------------|
| V_{dc} | dc-link voltage | 290 | [V] |
| T_s | Sampling time | 200 | [μ s] |
| f_s | Switching frequency | 5 | [kHz] |
| f_1 | Fundamental frequency | 60 | [Hz] |
| $V_{L,rms}$ | Load output voltage | 110 | [V] |
| L_f | Output filter inductance | 10 | [mH] |
| C_f | Output filter capacitance | 7 | [μ F] |
| R_L | Resistance for linear load | 60 | [Ω] |
| R_{load} | Resistance for nonlinear load | 200 | [Ω] |
| C_{load} | Capacitance for nonlinear load | 650 | [μ F] |
| L_{load} | Inductance for nonlinear load | 4 | [mH] |

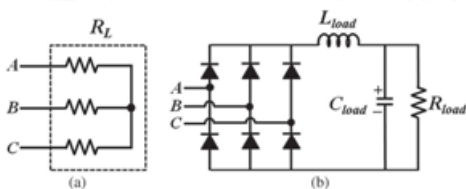


Fig. 4. Two types of load circuits. (a) Resistive linear load. (b) Nonlinear load with a three-phase diode rectifier.

VI. PERFORMANCE VALIDATIONS

A. Testbed Description

The proposed observer-based optimal voltage controller has been performed through both simulations with MATLAB/ Simulink and experiments with a prototype 600-VA UPS inverter testbed. Moreover, the conventional FLC scheme [17] is adopted to exhibit a comparative analysis of the proposed control scheme since it reveals a reasonable performance for nonlinear load and has the circuit model of a three-phase inverter similar to our system. Fig. 3 illustrates the overall block diagram to carry out the proposed algorithm using a 16-bit floating-point TMS320LF28335 DSP. In the testbed, the inverter phase currents and line-to-neutral load voltages are measured via the CTs and PTs to implement the feedback control. In this paper, a space vector PWM technique is used to generate the control inputs ($V_{i\alpha}$ and $V_{i\beta}$) in real time. Table I lists all system parameters used in this study.

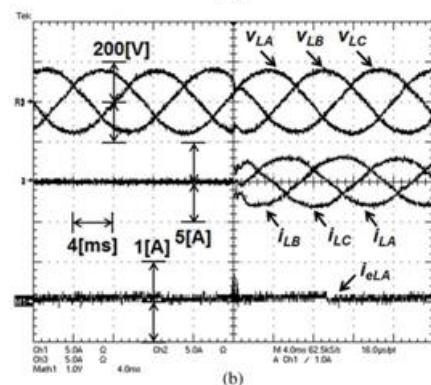
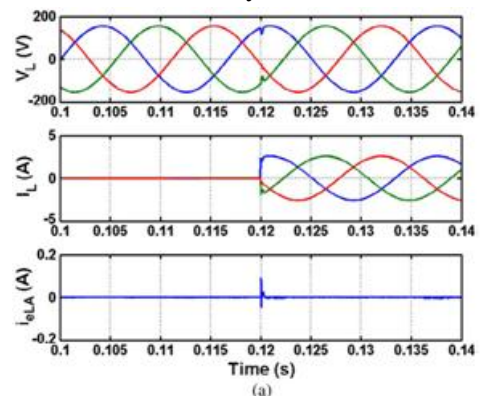


Fig. 5. Simulation and experimental results of the proposed observer based optimal voltage control scheme under load step change with $\pm 30\%$ parameter variations in L_f and C_f (i.e., balanced resistive load: 0%–100%)—First: Load output

voltages (VL), Second: Load output currents (IL),
 Third: Phase A load current error (ieLA=iLA
 -iLA). (a) Simulation. (b) Experiment.

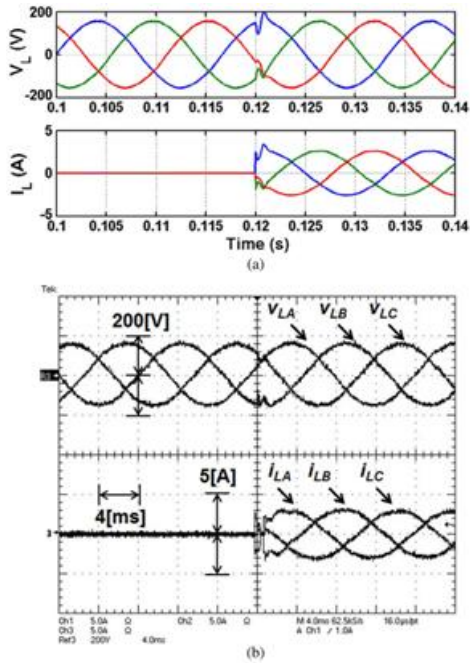


Fig. 6. Simulation and experimental results of the conventional FLC scheme under load step change with -30% parameter variations in Lf and Cf(i.e., balanced resistive load: 0%-100%)—First: Load output voltages (VL), Second: Load output currents (IL). (a) Simulation. (b) Experiment.

The proposed algorithm is verified through two different types of loads as explicitly depicted in Fig. 4. More specifically, Fig. 4(a) shows a linear-load circuit that consists of a resistor per phase, whereas Fig. 4(b) depicts a nonlinear-load circuit that is comprised of a three-phase full-bridge diode rectifier, an inductor (L_{load}), a capacitor (C_{load}), and a resistor (R_{load}). Note that during simulation and the experiment, observer gain L and controller gain K are selected based on Remark 1 as

$$L = 10^5 \begin{bmatrix} -1.0029 & 0.0003 \\ -0.0003 & -1.0029 \\ 1.1877 & 0 \\ 0 & 1.1877 \end{bmatrix}$$

$$K = 10^{11} \begin{bmatrix} 0.3241 & 0 & 3.1623 & 0 \\ 0 & 0.3241 & 0 & 3.1623 \end{bmatrix}$$

TABLEII: STEADY-STATE PERFORMANCES OF THE PROPOSED AND CONVENTIONAL SCHEMES

| Control Scheme | | The Proposed Observer-Based Optimal Voltage Control Scheme | | |
|-----------------------|------------|--|------------|-----------|
| Load Condition | | Step change | Unbalanced | Nonlinear |
| THD (%) | Simulation | 0.11 | 0.13 | 0.89 |
| | Experiment | 0.89 | 0.91 | 1.72 |
| Load RMS Voltages (V) | Simulation | v _{LA} | 109.9 | 109.6 |
| | | v _{LB} | 109.8 | 109.5 |
| | | v _{LC} | 110.0 | 109.8 |
| | Experiment | v _{LA} | 109.9 | 109.4 |
| | | v _{LB} | 109.9 | 109.5 |
| | | v _{LC} | 109.7 | 109.7 |
| Control Scheme | | The Conventional FLC Scheme | | |
| Load Condition | | Step change | Unbalanced | Nonlinear |
| THD (%) | Simulation | 0.94 | 0.97 | 1.96 |
| | Experiment | 1.32 | 1.39 | 2.98 |
| Load RMS Voltages (V) | Simulation | v _{LA} | 109.7 | 109.3 |
| | | v _{LB} | 110.0 | 109.3 |
| | | v _{LC} | 109.8 | 109.3 |
| | Experiment | v _{LA} | 109.8 | 109.3 |
| | | v _{LB} | 109.8 | 109.2 |
| | | v _{LC} | 109.7 | 109.3 |

B. Simulation and Experimental Results

The proposed voltage control calculation is done in different conditions (i.e., load step change, uneven burden, and nonlinear burden) to perfectly uncover its benefits. With a specific end goal to in a split second draw in and withdraw the heap amid a transient condition, the on-off switch is utilized as appeared in Fig. 3. The resistive burden portrayed in Fig. 4(a) is connected under both the heap step change condition (i.e., 0%-100%) and the uneven burden condition (i.e., stage B opened) to test the heartiness of the proposed plan when the heap is all of a sudden detached. In useful applications, the most well-known resilience varieties of the channel inductance (L_f) and channel capacitance (C_f), which are utilized as a yield channel, are inside ±10%. To promote legitimize the power under parameter varieties, a 30% decrease in both L_f and C_f is accepted under all heap conditions, for example, load step change, lopsided burden, and nonlinear burden. Fig. 5 demonstrates the reproduction and exploratory consequences of the proposed control strategy amid the heap step change. In addition, Fig. 6 exhibits the similar results got by utilizing the traditional FLC plan under the same condition.

In particular, the figures show the load voltages (First waveform: VL), load currents (Second waveform: IL), and stage A load current error (Third waveform: $i_{eLA} = i_{LA} - \hat{i}_{LA}$). Note that the load current error waveform in the consequences of the ordinary FLC technique is excluded on the grounds that the FLC plan does not require load current data. It can be seen in Fig. 5 that when the load is all of a sudden changed, the load yield voltage displays little mutilation. However, it rapidly comes back to a consistent state condition in 1.0 ms, as shown in the reenactment brings about Fig. 5(a).

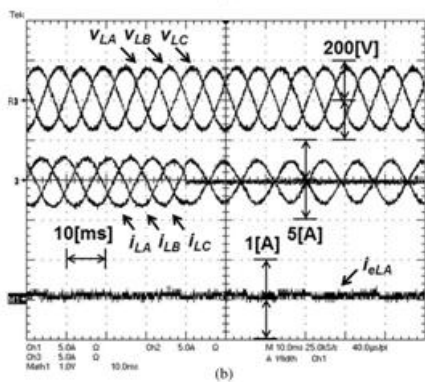
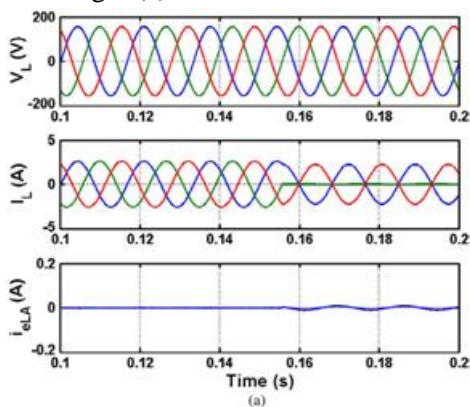


Fig. 7. Simulation and experimental results of the proposed observer based optimal voltage control scheme under unbalanced load with -30% parameter variations in L_f and C_f (i.e., phase B opened)—First: Load output voltages (VL), Second: Load output currents (IL), Third: Phase A load current error ($i_{eLA} = i_{LA} - \hat{i}_{LA}$). (a) Simulation. (b) Experiment.

Moreover, it has revealed a fast recovery time of 1.5 ms in a real experimental setup as shown in Fig. 5(b).

Conversely, as illustrated in the simulation results in Fig. 6(a), voltage distortion is larger, and its recovery time of 1.4 ms is much longer as compared with that in Fig. 5(a). Moreover, Fig. 6(b) shows a longer recovery time of 2.0 ms than that observed in Fig. 5(b). On the other hand, the THD values of the load output voltage at steady-state full-load operation are presented in Table II. These values are found as 0.11% for simulation and 0.89% for experiment using the proposed scheme. However, the conventional FLC scheme shows 0.94% and 1.32% for the case of simulation and experiment, respectively. Therefore, it is explicitly demonstrated that the proposed algorithm attains lower THD. It can be observed from Table II that the load root mean square (RMS) voltage values in both schemes are appropriately regulated at steady state. Moreover, the third waveform in Fig. 5 shows a small load current error (i_{eLA}) between the measured value (i_{LA}) and the estimated value (\hat{i}_{LA}).

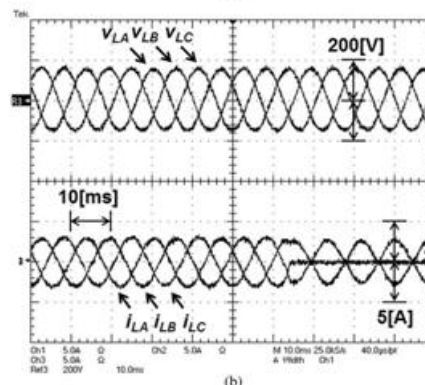
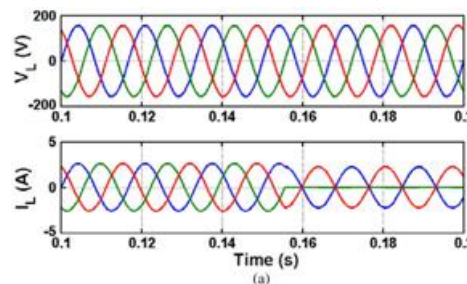


Fig. 8. Simulation and experimental results of the conventional FLC scheme under unbalanced load with -30% parameter variations in L_f and C_f (i.e., phase B opened) First: Load output voltages (VL), second: Load output currents (IL). (a) Simulation. (b) Experiment.

Next, the characteristic performances of the transient and steady state under unbalanced load are verified through Figs. 7 and 8. Precisely, this case is implemented under a full-load condition by suddenly opening phase B. It is shown that the load output voltages are controlled well, although the rapid change in the heap current of stage B is seen as it is opened. As appeared in Fig. 7, the particular THD estimations of the yield voltage are 0.13% for the reproduction and 0.91% for the examination got by utilizing the proposed technique. Be that as it may, the THD qualities are 0.97% and 1.39%, separately, for the reenactment and investigation if there should arise an occurrence of the routine FLC plan, as delineated in Fig. 8. As given in Table II, little relentless state voltage blunders under lopsided burden are watched on the grounds that the heap RMS voltage estimations of both techniques are right around 110 V. Furthermore, the heap current spectator gives top notch data to the proposed controller as depicted in Fig. 7. To assess the relentless state execution under nonlinear burden, a three-stage diode rectifier appeared in Fig. 4(b) is utilized. The recreation and exploratory aftereffects of every control technique under this condition are shown in Figs. 9 and 10. To this end, the THD estimations of the heap voltage waveforms accomplished with the proposed plan are 0.89% for recreation and 1.72% for examination, individually. On account of the ordinary FLC plan, the comparing load voltage THD qualities are 1.96% for recreation and 2.98% for examination, individually. It can be likewise watched that the proposed control technique gives a superior burden voltage direction in consistent state contrasted and the customary FLC strategy. In Fig. 9, it can be clearly seen that the heap current onlooker ensures a decent estimation for each formance as a result of a little load current mistake (i_{eLA}). At long last, all THD and burden RMS voltage values under the three burden conditions already portrayed are condensed in Table II.

VII. CONCLUSION:

This paper has proposed a basic spectator based ideal voltage control strategy for the three-stage UPS frameworks.

The proposed controller is made out of a criticism control term to balance out the blunder progression of the framework and a remunerating control term to gauge the framework instabilities. In addition, the ideal burden current spectator was utilized to improve framework expense and dependability. This paper demonstrated the shut circle security of a spectator based ideal voltage controller by utilizing the Lyapunov hypothesis. Moreover, the proposed voltage control law can be deliberately planned considering a tradeoff between control info greatness and following mistake dissimilar to past calculations. The prevalent execution of the proposed control framework was exhibited through recreations and investigations. Under three burden conditions (load step change, uneven burden, and nonlinear burden), the proposed control plan uncovered a superior voltage following execution, for example, lower THD, littler consistent state blunder, and quicker transient reaction than the traditional FLC conspire regardless of the possibility that there exist parameter varieties.

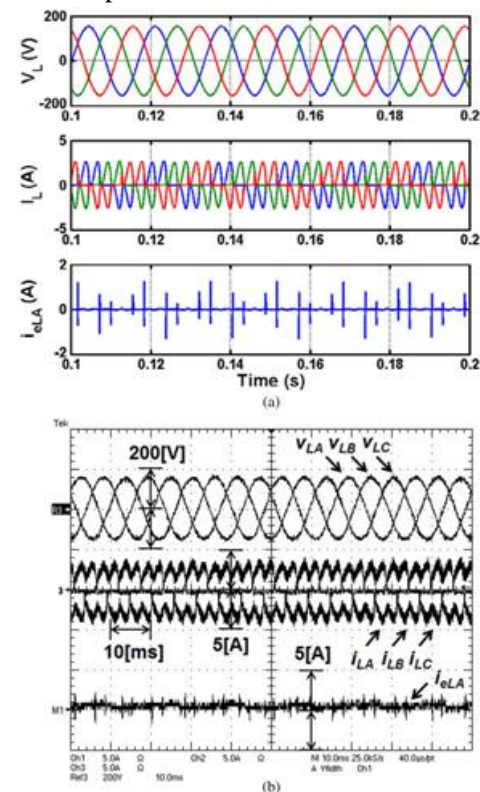


Fig. 9. Simulation and experimental results of the proposed observer based optimal voltage control

scheme under nonlinear load with -30% parameter variations in Lf and Cf(i.e., three-phase diode rectifier)—First: Load output voltages (VL), Second: Load output currents (IL), Third: Phase A load current error (ieLA= iLA - îLA).(a) Simulation. (b) Experiment.

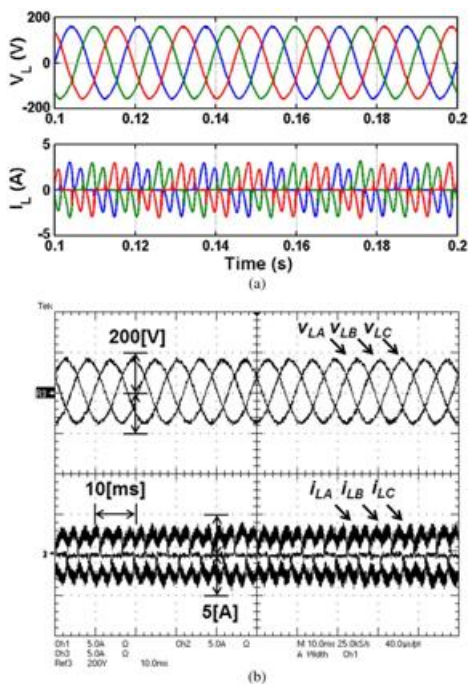


Fig. 10. Simulation and experimental results of the conventional FLC scheme under nonlinear load with -30% parameter variations in Lf and Cf(i.e., three-phase diode rectifier)—First: Load output voltages (VL), Second: Load output currents (IL). (a) Simulation. (b) Experiment.

REFERENCES

[1]A. Nasiri, “Digital control of three-phase series-parallel uninterruptible power supply systems,” IEEE Trans. Power Electron., vol. 22, no. 4, pp. 1116–1127, Jul. 2007.

[2]Y. H. Chen and P. T. Cheng, “An inrush current mitigation technique for the line-interactive uninterruptible power supply systems,” IEEE Trans.Ind. Appl., vol. 46, no. 4, pp. 1498–1508, May/June. 2010.

[3]K. S. Low and R. Cao, “Model predictive control of parallel-connected inverters for uninterruptible power supplies,” IEEE Trans. Ind. Electron., vol. 55, no. 8, pp. 2884–2893, Aug. 2008.

[4]A. Mokhtarpour, H. A. Shayanfar, M. Bathaee, and M. R. Banaei, “Control of a single phase unified power quality conditioner-distributed generation based input output feedback linearization,” J. Elect. Eng. Technol., vol. 8, no. 6, pp. 1352–1364, Nov. 2013.

[5]J. H. Lee, H. G. Jeong, and K. B. Lee, “Performance improvement of grid-connected inverter systems under unbalanced and distorted grid voltage by using a PR controller,” J. Elect. Eng. Technol., vol. 7, no. 6, pp. 918–925, Nov. 2012.

[6] H. K. Kang, C. H. Yoo, I. Y. Chung, D. J. Won, and S. I. Moon, “Intelligent coordination method of multiple distributed resources for harmonic current compensation in a microgrid,” J. Elect. Eng. Technol., vol. 7, no. 6, pp. 834–844, Nov. 2012.

[7] C. Salim, B. M. Toufik, and G. Amar, “Harmonic current compensation based on three-phase three-level shunt active filter using fuzzy logic current controller,” J. Elect. Eng. Technol., vol. 6, no. 5, pp. 595–604, Sep. 2011.

[8] U. Borup, P. N. Enjeti, and F. Blaabjerg, “A new space-vector-based control method for UPS systems powering nonlinear and unbalanced loads,” IEEE Trans. Ind. Appl., vol. 37, no. 6, pp. 1864–1870, Nov./Dec. 2001.

[9] H. Karimi, A. Yazdani, and R. Iravani, “Robust control of an autonomous four-wire electronically-coupled distributed generation unit,” IEEE Trans.Power Del., vol. 26, no. 1, pp. 455–466, Jan. 2011.

- [10] T. S. Lee, S. J. Chiang, and J. M. Chang, “ H_{∞} loop-shaping controller designs for the single-phase UPS inverters,” *IEEE Trans. Power Electron.*, vol. 16, no. 4, pp. 473–481, Jul. 2001.
- [11] P. Cortés et al., “Model predictive control of an inverter with output LC filter for UPS applications,” *IEEE Trans. Ind. Electron.*, vol. 56, no. 6, pp. 1875–1883, Jun. 2009.
- [12] T. Kawabata, T. Miyashita, and Y. Yamamoto, “Dead beat control of three phase PWM inverter,” *IEEE Trans. Power Electron.*, vol. 5, no. 1, pp. 21–28, Jan. 1990.
- [13] H. Komurcugil, “Rotating sliding line based sliding mode control for single-phase UPS inverters,” *IEEE Trans. Ind. Electron.*, vol. 59, no. 10, pp. 3719–3726, Oct. 2012.
- [14] O. Kukrer, H. Komurcugil, and A. Doganalp, “A three-level hysteresis function approach to the sliding mode control of single-phase UPS inverters,” *IEEE Trans. Ind. Electron.*, vol. 56, no. 9, pp. 3477–3486, Sep. 2009.
- [15] G. Escobar, A. A. Valdez, J. Leyva-Ramos, and P. Mattavelli, “Repetitive-based controller for a UPS inverter to compensate unbalance and harmonic distortion,” *IEEE Trans. Ind. Electron.*, vol. 54, no. 1, pp. 504–510, Feb. 2007.
- [16] T. D. Do, V. Q. Leu, Y. S. Choi, H. H. Choi, and J. W. Jung, “An adaptive voltage control strategy of three-phase inverter for stand-alone distributed generation systems,” *IEEE Trans. Ind. Electron.*, vol. 60, no. 12, pp. 5660–5672, Dec. 2013.
- [17] D. E. Kim and D. C. Lee, “Feedback linearization control of three-phase,” *IEEE Trans. Ind. Electron.*, vol. 57, no. 3, pp. 963–968, Mar. 2010.
- [18] T. D. Do, S. Kwak, H. H. Choi, and J. W. Jung, “Suboptimal control scheme design for interior permanent-magnet synchronous motors: An SDRE-based approach,” *IEEE Trans. Power Electron.*, vol. 29, no. 6, pp. 3020–3031, Jul. 2013.
- [19] F. Lin, *Robust Control Design: An Optimal Control Approach*. Chichester, U.K.: Wiley, 2007.
- [20] C. Olalla, R. Leyva, A. E. Aroudi, and I. Queinnec, “Robust LQR control for PWM converters: An LMI approach,” *IEEE Trans. Ind. Electron.*, vol. 56, no. 7, pp. 2548–2558, Jul. 2009.
- [21] P. Rao, M. L. Crow, and Z. Yang, “STATCOM control for power system voltage control applications,” *IEEE Trans. Power Del.*, vol. 15, no. 4, pp. 1311–1317, Oct. 2000.
- [22] Y. S. Rao and M. C. Chandokar, “Real-time electrical load emulator using optimal feedback control technique,” *IEEE Trans. Ind. Electron.*, vol. 57, no. 4, pp. 1217–1225, Apr. 2010.
- [23] T. Cimen, “State-dependent Riccati equation control: A survey,” in *Proc. IFAC World Congr.*, Seoul, Korea, Jul. 2008, vol. 17, pp. 3761–3775.
- [24] H. Tao, J. L. Duarte, and M. A. M. Hendrix, “Line-interactive UPS using a fuel cell as the primary source,” *IEEE Trans. Ind. Electron.*, vol. 55, no. 8, pp. 3012–3021, Aug. 2008.